Monolayer polar metals with large piezoelectricity derived from $MoSi_2N_4$

Yan Yin,[†] Qihua Gong,[*,†,‡] Min Yi,[*,†] and Wanlin Guo[†]

†*State Key Laboratory of Mechanics and Control for Aerospace Structures & Key Laboratory for Intelligent Nano Materials and Devices of Ministry of Education & Institute for Frontier Science & College of Aerospace Engineering, Nanjing University of Aeronautics and Astronautics (NUAA), Nanjing 210016, China*

‡*MIIT Key Laboratory of Aerospace Information Materials and Physics & College of Physics, Nanjing University of Aeronautics and Astronautics (NUAA), Nanjing 211106, China*

E-mail: gongqihua@nuaa.edu.cn; yimin@nuaa.edu.cn

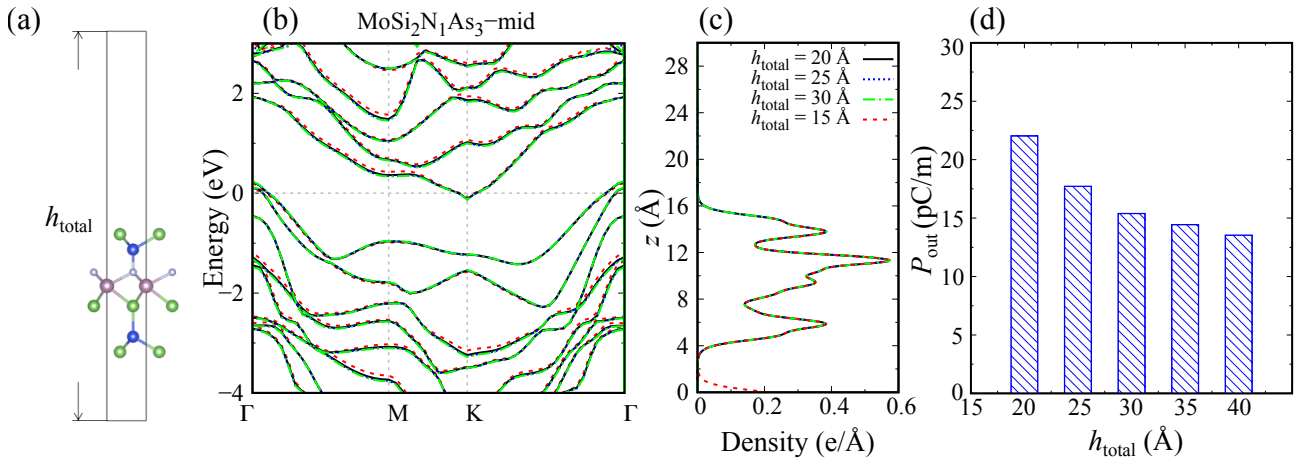

Fig. S1. (a) Side view of the lattice structure of $MoSi_2N_1As_3$-mid monolayer. h_{total} is the total thickness, including the layer and vacuum thickness. Effect of vacuum thickness on the (a) band structure, (b) planar-average charge density along z-direction (ρ_z), and (c) out-of-plane polarization (P_{out}) of $MoSi_2N_1As_3$-mid monolayer. When $h_{total} \leq 20$ Å (i.e., $h_{total} = 15$ Å), the influence of periodic boundary condition is significant on the band structure and ρ_z. When $h_{total} \geq 20$ Å, the curves of band structure coincide completely, as well as the curves of ρ_z. P_{out} tends to the convergence until $h_{total} = 40$ Å. These indicate that the sufficient vacuum thickness is necessary for the calculation of $MoSi_2N_xZ_{4-x}$ monolayer, which is set to more than 20 Å in this paper.

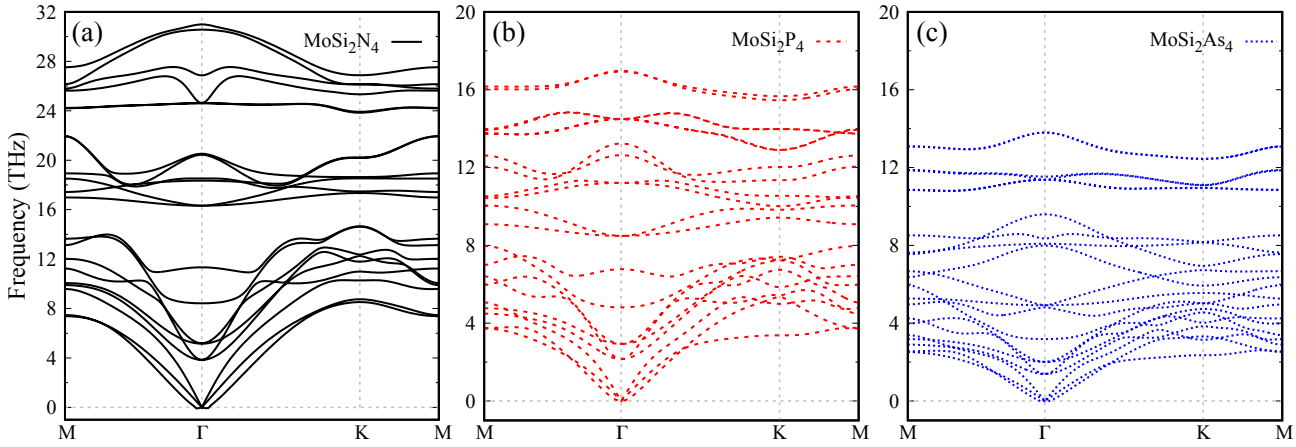

Fig. S2. Phonon dispersion spectra of (a) $MoSi_2N_4$, (b) $MoSi_2P_4$ and (c) $MoSi_2As_4$.

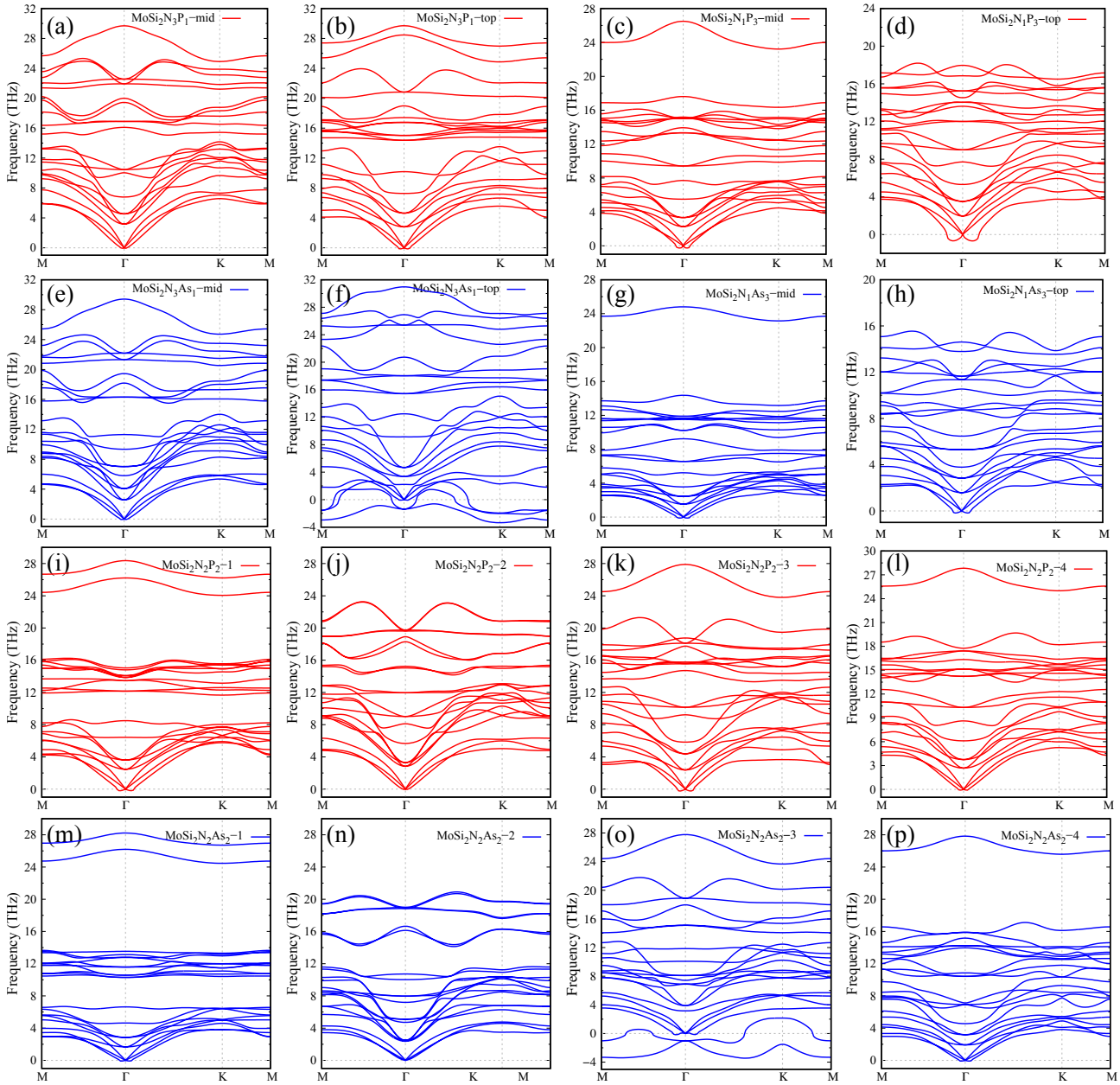

Fig. S3. Phonon dispersion spectra of $MoSi_2N_xZ_{4-x}$ monolayers.

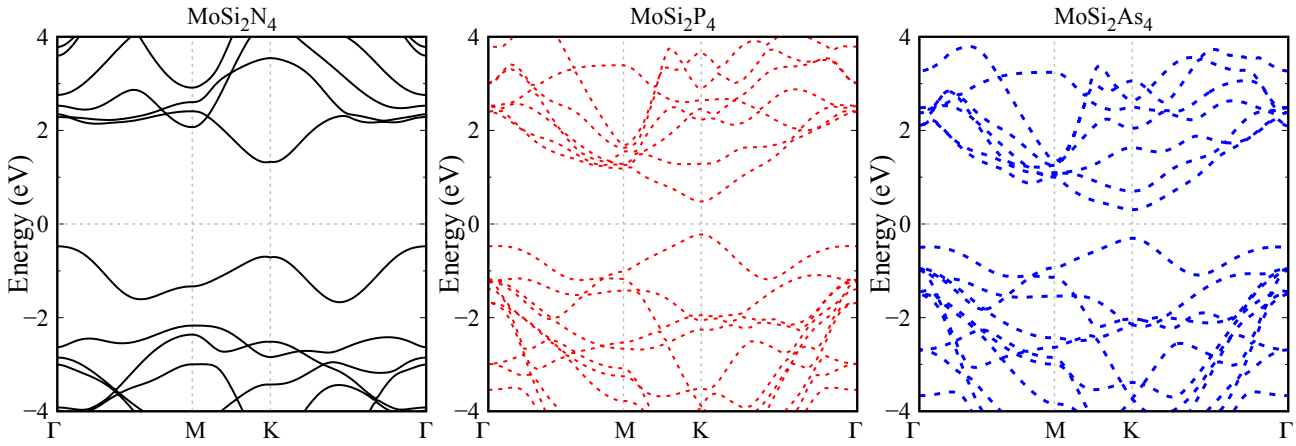

Fig. S4. Band structures of $MoSi_2X_4$ (X=N/P/As).

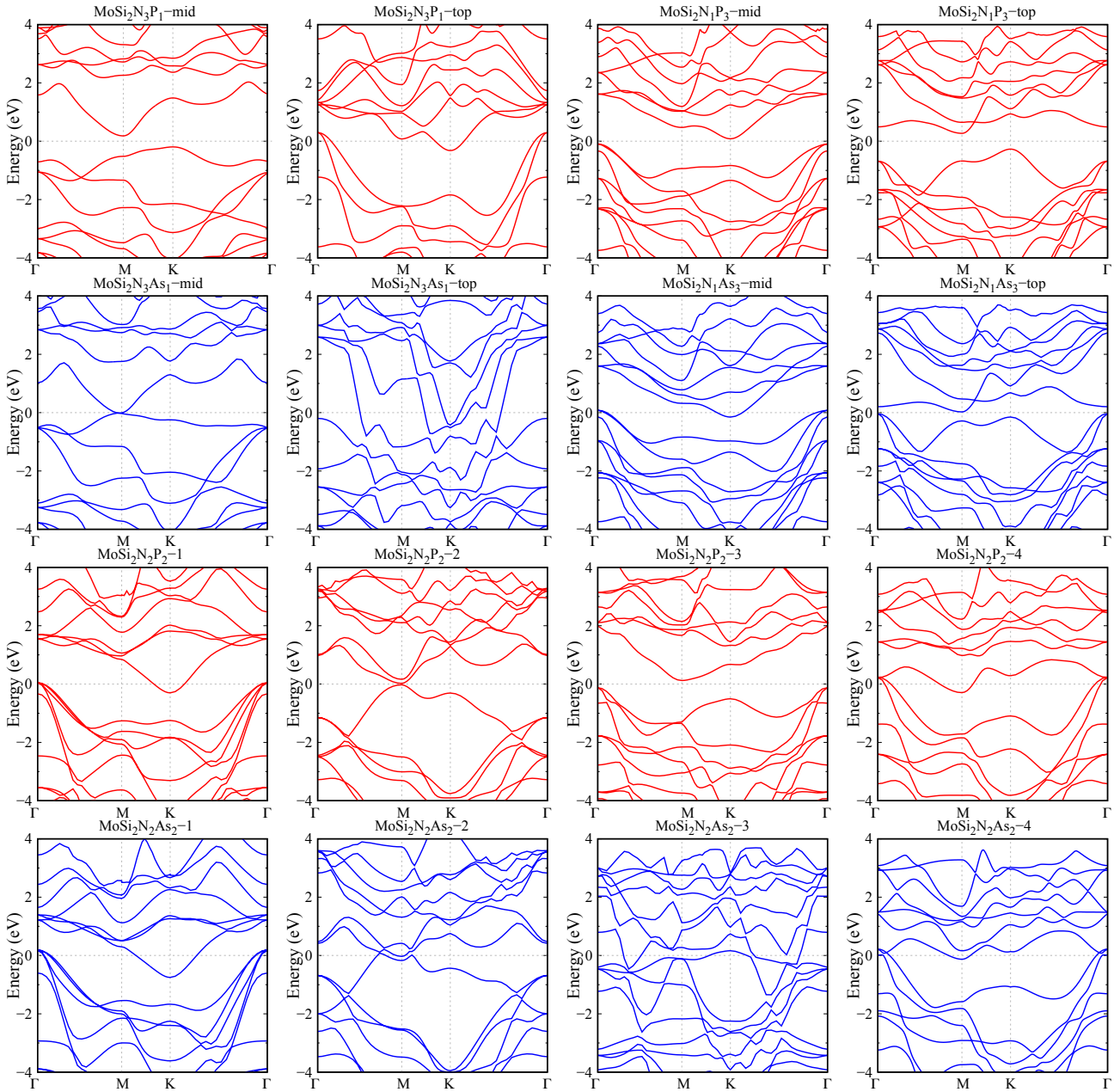

Fig. S5. Band structures of $MoSi_2N_xZ_{4-x}$ monolayers.

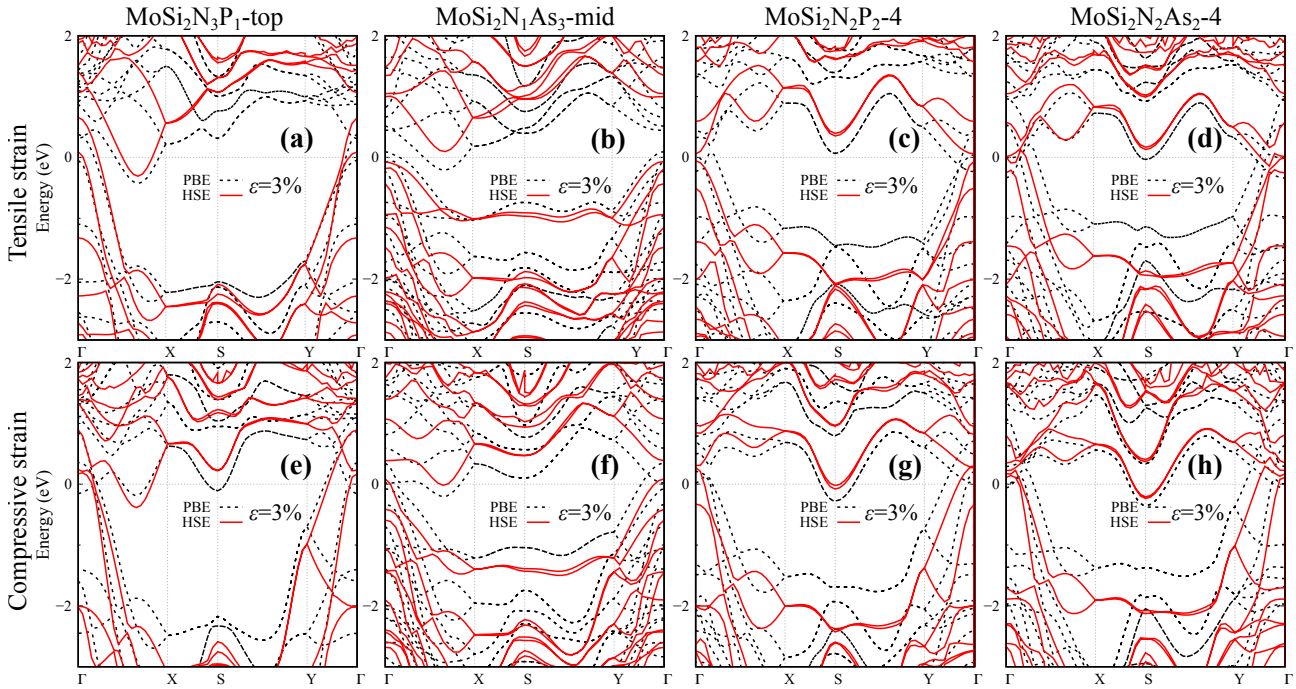

Fig. S6. Band structures of $MoSi_2N_3P_1$-top, $MoSi_2N_1As_3$-mid, $MoSi_2N_2P_2$-4, and $MoSi_2N_2As_2$-4 under zigzag uniaxial strain: (a)–(d) tensile strain of 3%, (e)–(h) compressive strain of 3%. The dash and red solid lines are the results calculated by PBE and HSE, respectively. $MoSi_2N_3P_1$-top and $MoSi_2N_2As_2$-4 are metals under both tensile and compressive strains. $MoSi_2N_1As_3$-mid and $MoSi_2N_2P_2$-4 are metals under a compressive strain, but semiconductors under a tensile strain, indicating the adjustability of band structure under a tensile strain.

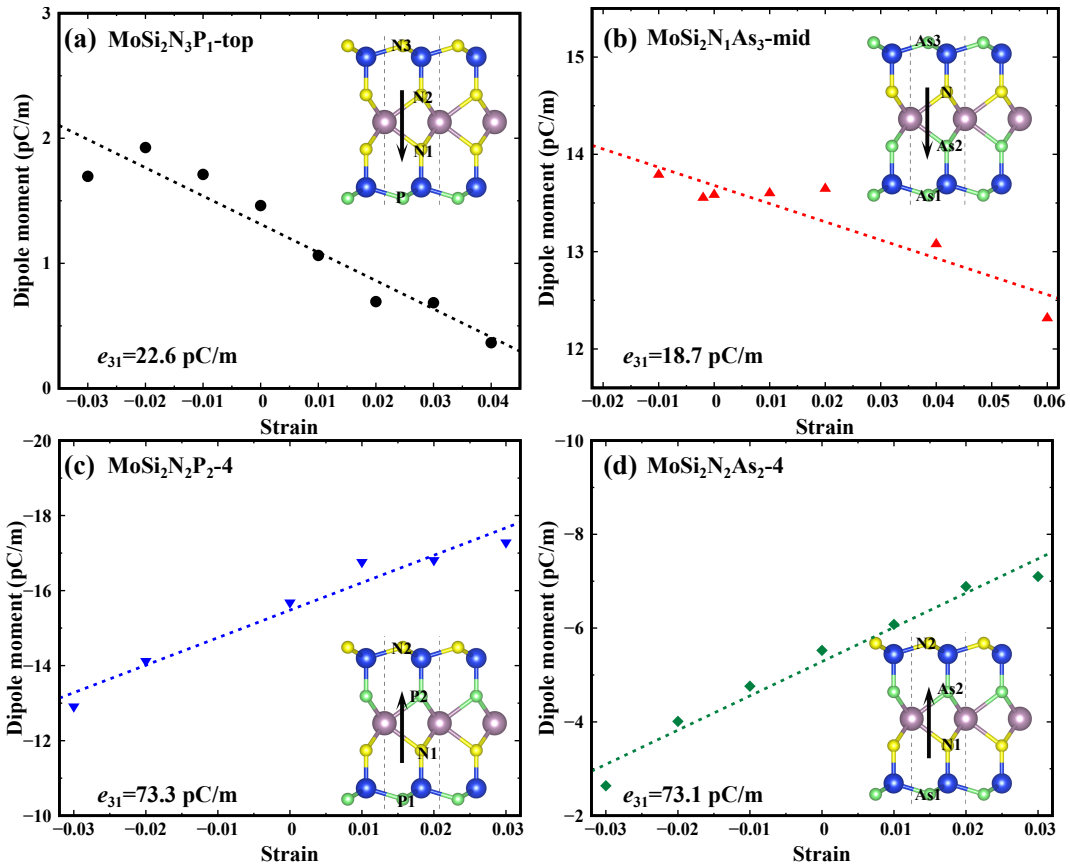

Fig. S7. OOP dipole moment as a function of zigzag uniaxial strain: (a) $MoSi_2N_3P_1$-top, (b) $MoSi_2N_1As_3$-mid, (c) $MoSi_2N_2P_2$-4, (d) $MoSi_2N_2As_2$-4. The inset arrows indicate the dipole moment direction.

Table S1. Out-of-plane polarizations (P_{out}) of several 2D semiconductors calculated by the method based on the classical electrodynamics and Berry phase.

Structure	P_{out} (eÅ/u.c.)	
	Berry phase	Classical eletrodynamics
In_2Se_3	0.18 [1]	0.094–0.11 [2,3]
$CrSe_2$	0.033 [4]	0.033 [4]
MnS_2	–0.054 [4]	–0.054 [4]
$MnSe_2$	–0.046 [4]	–0.046 [4]
$NbSe_2$	0.087 [4]	0.088 [4]
VS_2	0.099 [4]	0.099 [4]
VSe_2	0.066 [4]	0.066 [4]

Table S2. Structrual parameters of $MoSi_2N_xZ_{4-x}$ monolayers, i.e., lattice constants, thickness (h), bond length, cohesive energy (E_{coh}), enthalpy of formation (E_F), dynamical stability and band gap from PBE (E_g^{PBE}) and HSE (E_g^{HSE})

Structure	$a = b$ (Å)	h (Å)	d_{Z4-Si2} (Å)	d_{Z3-Si2} (Å)	d_{Z3-Mo} (Å)	d_{Z2-Mo} (Å)	d_{Z2-Si1} (Å)	d_{Z1-Si1} (Å)	E_{coh} (eV/atom)	E_F (eV/atom)	Dynamics (Y/N)	E_g^{PBE} (eV)	E_g^{HSE} (eV)
$MoSi_2N_4$	2.91	10.01	1.76	1.75	2.10	2.10	1.75	1.76	-8.59	-0.94	Y	1.79	*
$MoSi_2P_4$	3.47	13.17	2.25	2.24	2.46	2.46	2.24	2.25	-6.29	-0.34	Y	0.70	*
$MoSi_2As_4$	3.62	13.94	2.37	2.36	2.56	2.56	2.36	2.37	-5.67	-0.09	Y	0.56	*
$MoSi_2N_3P_1$-mid	2.98	10.92	1.79	2.23	2.37	2.12	1.75	1.79	-7.94	-0.28	Y	0.38	0.96
$MoSi_2N_3P_1$-top	3.05	10.95	2.15	1.73	2.14	2.13	1.75	1.82	-7.73	-0.49	Y	*	*
$MoSi_2N_2P_2$-1	3.23	11.71	2.18	1.75	2.21	2.21	1.75	2.18	-7.05	-0.24	Y	*	*
$MoSi_2N_2P_2$-2	3.05	11.72	1.83	2.23	2.38	2.38	2.23	1.83	-7.34	-0.53	Y	0.05	0.63
$MoSi_2N_2P_2$-3	3.14	11.66	1.87	1.76	2.16	2.39	2.23	2.16	-7.20	-0.39	Y	0.24	0.88
$MoSi_2N_2P_2$-4	3.15	11.67	1.86	2.25	2.39	2.17	1.73	2.17	-7.17	-0.37	Y	*	*
$MoSi_2N_1P_3$-mid	3.33	12.34	2.20	1.75	2.23	2.42	2.24	2.21	-6.65	-0.27	Y	0.18	0.40
$MoSi_2N_1P_3$-top	3.26	12.33	1.93	2.24	2.42	2.42	2.23	2.19	-7.72	-1.35	N	0.54	0.58
$MoSi_2N_3As_1$-mid	2.99	11.15	1.80	2.35	2.47	2.12	1.75	1.79	-7.70	-0.56	Y	0.01	0.48
$MoSi_2N_3As_1$-top	2.88	12.63	1.74	1.74	2.09	2.09	1.78	3.13	-7.59	-0.46	N	*	*
$MoSi_2N_2As_2$-1	3.31	12.05	2.30	1.73	2.23	2.23	1.733	2.30	-6.66	-0.04	Y	*	*
$MoSi_2N_2As_2$-2	3.08	12.21	1.83	2.36	2.48	2.48	2.36	1.83	-6.90	-0.28	Y	*	*
$MoSi_2N_2As_2$-3	3.11	12.42	1.85	1.75	2.14	2.49	2.37	2.38	-6.41	0.21	N	*	*
$MoSi_2N_2As_2$-4	3.20	12.04	1.89	2.38	2.49	2.18	1.71	2.29	-6.76	-0.14	Y	*	*
$MoSi_2N_1As_3$-mid	3.49	12.77	2.34	1.74	2.27	2.54	2.36	2.33	-6.15	-0.05	Y	*	*
$MoSi_2N_1As_3$-top	3.35	12.88	1.97	2.37	2.49	2.51	2.34	2.30	-6.13	-0.03	Y	0.04	0.52

References

(1) Chen, Y.; Tang, Z.; Shan, H.; Jiang, B.; Ding, Y.; Luo, X.; Zheng, Y. Enhanced out-of-plane piezoelectric effect in In_2Se_3/transition metal dichalcogenide heterostructures. *Physical Review B* **2021**, *104*, 075449.

(2) Ding, W.; Zhu, J.; Wang, Z.; Gao, Y.; Xiao, D.; Gu, Y.; Zhang, Z.; Zhu, W. Prediction of intrinsic two-dimensional ferroelectrics in In_2Se_3 and other III_2-VI_3 van der Waals materials. *Nature Communications* **2017**, *8*, 14956.

(3) Zhang, L.; Tang, C.; Zhang, C.; Du, A. First-principles screening of novel ferroelectric MXene phases with a large piezoelectric response and unusual auxeticity. *Nanoscale* **2020**, *12*, 21291–21298.

(4) Li, Y.; Legut, D.; Liu, X.; Lin, C.; Feng, X.; Li, Z.; Zhang, Q. Modulated ferromagnetism and electric polarization induced by surface vacancy in MX_2 monolayers. *Journal of Physical Chemistry C* **2022**, *126*, 8817–8825.